JACS
JOURNAL OF THE AMERICAN CHEMICAL SOCIETY

ARTICLE

pubs.acs.org/JACS

# Stereoselective Cycloaddition of 1,3-Cyclohexadiene on Si(100): A Simple Algorithm for Product Identification Based on Secondary Orbital Interactions

Peter M. Ryan,[†,‡] Lucile C. Teague,[†,¶] David E. Meehan,[†] and John J. Boland[*,†]

[†]School of Chemistry and Centre for Research on Adaptive Nanostructures and Nanodevices (CRANN), Trinity College Dublin, Dublin 2, Ireland

[‡]National Institute for Nanotechnology,11421 Saskatchewan Drive, Edmonton, Alberta, Canada

[¶]Savannah River National Laboratory, Aiken, South Carolina, United States

Supporting Information

**ABSTRACT:** We consider the reaction of 1,3-cyclohexadiene (1,3-CHD) on Si(100) and show that the observed reactivity and stereoselectivity cannot be explained on the basis of thermodynamics. We postulate the existence of secondary orbital interactions (SOIs) and introduce a simple algorithm that examines all possible secondary interactions between the frontier orbitals of the molecule and the surface. We demonstrate using an orbital symmetry-based algorithm supported by DFT calculations that SOIs favor a particular molecular configuration, consistent with the experimental observations. The potential role of SOIs in controlling surface chemical reactions is discussed.

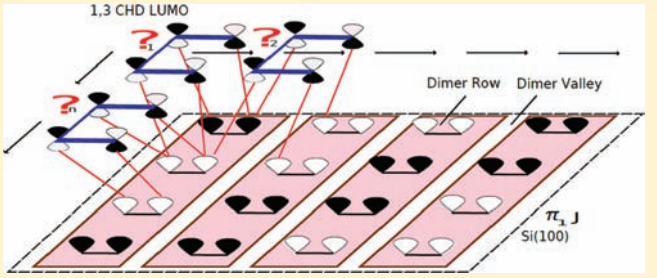


Previous STM and FTIR studies of the reactions of a variety of small, conjugated molecular systems on the Si(100)-2 × 1 and Ge(100)-2 × 1 surfaces have collectively revealed product distributions inconsistent with those predicted by the traditional Woodward−Hoffmann rules for concerted cycloaddition reactions.[1−3] Furthermore, for several of these systems, comparison between the experimental results and theoretically predicted products suggest that kinetics, rather than thermodynamics, plays an important role in the observed product distributions.[4−10] Although numerous experimental and theoretical studies have been completed for these types of surface reactions, the specific mechanisms that lead to the observed surface reactivity and product selectivity are still being debated. To that end, we discuss the role of secondary orbital interactions (SOIs) in determining the product distribution and selectivity observed for the reaction of 1,3-cyclohexadiene with the Si(100)-2 × 1 surface.

Since first postulated by Woodward and Hoffman ca. 1965,[11,12] the concept of secondary orbital interactions has been used extensively to explain facile steroselectivity in Diels−Alder type reactions. Generally, the concept involves accounting for the energetic contributions to a sterodefining transition state brought about by bonding and antibonding overlap between the frontier orbitals of each reacting moiety. According to Woodward−Hoffmann analysis, SOIs lower the energy of one transition state relative to another where this interaction is either unfavorable or absent. Using such arguments they explained why, for instance, a higher energy steroisomer might be kinetically favored above the true thermodynamic product. While the concept of SOI is now deeply embedded in organic chemistry it has, to the best of our knowledge, never been invoked to explain steroselectivity within a heterogeneous reaction. In particular, we make use of our recently published DFT and Brillouin zone folding technique[13] that generates the full set of high symmetry crystal wave functions (CWs) appropriate to the ground state Si(100) c(4 × 2) surface. Using these results we introduce a simple algorithm based on the conservation of orbital symmetry that identifies possible frontier orbital interactions on the endo and exo reaction trajectories. We demonstrate with the aid of DFT that SOIs stabilize the transition state en route to exo product formation, and that this assignment is consistent with a careful re-examination of the original STM data.

Here, we consider the reaction of 1,3-cyclohexadiene (1,3-CHD) on Si(100) and propose that SOIs are responsible for the observed surface reactivity and selectivity. In our previous scanning tunneling microscopy (STM) and density functional theory (DFT) studies,[6,7] we identified the dominant species as the interdimer product involving reaction with adjacent dimers in the same row. DFT calculations have shown that there are two possible structural isomers for this product, i.e., the endo or exo products, which are very close in energy. Here, the endo−exo nomenclature is used specifically to denote the position of the remaining C═C double bond as being either over the Si dimer row (endo) or outside the dimer row (exo) (see Figure 1).

**Received:** December 22, 2010
**Published:** July 12, 2011

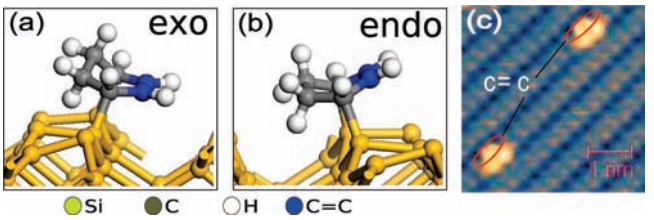


**Figure 1.** Molecular models of the (a) exo and (b) endo configurations for 1,3-CHD adsorption on Si(100). (c) Empty state STM image of 1,3-CHD dominant product on Si(100). In ref 7 the STM LDOS feature is tentatively identified as resulting from a [4 + 2]-like cycloaddition product configuration.

Experimentally, however, only a single product is observed, and our objective here is to explain the observed stereoselectivity.

In earlier STM and DFT studies of Teague et al.[6,7] five major reaction products for the attachment of 1,3-CHD to the Si(100) surface were identified. The dominant product (30% of all reacted species) is displayed in Figure 1c. Teague et al. used the registry of the C═C bond LDOS feature (imaged in empty-states as a short and symmetric double node) with respect to the Si dimers LDOS feature to aid in this identification. With this in mind, the empty state molecular feature in Figure 1c is seen to be comprised of a short nodal feature associated with the remaining C═C bond of the adsorbed 1,3-CHD molecule and another longer nodal feature associated with the two dangling bonds on the two adjacent surface Si atoms. Given this apparent registry and the fact the entire feature is symmetric about two Si dimers along the dimer row, Teague et al.,[6,7] tentatively identified the adsorption configuration as the endo cycloaddition product (see Figure 1b).

To assess the energetic differences between the endo and exo configurations in Figure 1, we used geometry optimizations enabled under the CASTEP[14] package. Calculations began with the generation of an appropriate substrate model to simulate the molecule−surface interaction while ensuring that possible adsorbate−adsorbate interactions across periodic supercells were minimized. In this respect, we represented the c(4 × 2) Si(100) surface with a rombohedral slab that contains in total four repeat units of the c(4 × 2) Si(100) surface unit cell. The model comprises 12 Si layers in the supercell with a vacuum separation of ∼20 Å. The four central Si layers were constrained to their bulk positions during the geometry optimization, and the dimers on the underside of the slab were capped with H atoms. This particular supercell was chosen because of its known ability to accurately return the full set of high symmetry CW's associated with the c(4 × 2) Si(100) surface using just a Γ-point sampling of the surface Brillouin zone.[13] Following optimization of this structure the unreacted 1,3-CHD molecule was imported into the supercell and positioned parallel to the Si (100) surface ∼3 Å above the central dimers of a single Si dimer row in either the endo or exo orientation. These two configurations were then subject to further geometry optimizations. Note that full details of the cells used and DFT convergence criteria are given in the Supporting Information (SI) section. The relative difference in energies between the optimized endo and exo adsorption configurations output from these calculations are presented in Table 1 where the fourth column reports the expected Boltzmann population ratio assuming the product distribution is determined solely by the thermodynamic energy differences. The results of this DFT analysis show that the exo product is stabilized over the endo product by ∼0.02 eV (or 0.46 kcal/mol) with an expected exo:endo population of about 2:1.

**Table 1. Energetic Data from the CASTEP Geometry Optimized Configurations of the Endo and Exo Configurations (see SI for details)**

| configuration | ΔE (eV) | ΔE (kcal/mol) | pop |
|---|---|---|---|
| exo | 0 | 0 | 2 |
| endo | 0.02 | 0.46 | 1 |

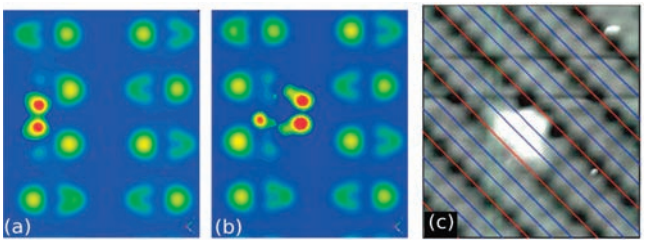


**Figure 2.** (a) and (b) Respective simulated STM images for the endo and exo adsorption configurations of 1,3 CHD on Si(100) generated from the empty state wave functions output from the DFT calculations. The C═C $\pi^*$ LDOS registry in the exo simulated STM image (b) is consistent with the actual STM data. (c) STM image ($V$ = +1.2, $I_t$ = 0.5 nA) (25 nm × 25 nm) of the dominant interdimer intrarow product on Si(100) surface following reaction of 1,3-CHD. The blue lines are drawn along the maxima of the silicon atoms that comprise the dimer rows, whereas the red lines represent the periodicity along the dimerization direction of the surface.

The DFT analysis outlined above also enabled us to calculate the surface LDOS associated with the endo and exo products so as to simulate the respective STM images. This was accomplished by summing the empty state wave functions associated with each optimized configuration over an energy interval from the Fermi energy to +3.5 eV. We note that the width of of the energy window in the LDOS summation is purposely expanded over the LDOS range sampled in the actual STM experiment. This step is taken to capture the computed LDOS associated with the C═C $\pi^*$ bond which has been shown, in the presence of a W tip, to be a major contributer to empty state STM images of the molecule at lower bias (2 eV).[13,15] Each simulated STM image (see Figure 2a and b) is then constructed by the superposition of two LDOS contour slices taken ∼1 Å above the Si(100) surface and ∼1 Å above the molecule, respectively. Figure 2a shows, for the simulated STM image corresponding to the endo configuration of the molecular adduct, that the dual node C═C intensity is located well inside the dimer row, whereas in the exo configuration of Figure 2b this feature is positioned between the dimer rows. The LDOS feature that appears above the dimer row in Figure 2b is a consequence of the uppermost LDOS slice intersecting a C−H bond on the underside of the molecular adduct and is unlikely to contribute to the experimental STM image. Figure 2c is a carefully constructed registry map of the experimental data where the blue lines are drawn along the maxima of the silicon atoms that comprise the dimer rows, whereas the red lines represent the periodicity along the dimerization direction of the surface. Distances between the blue and red lines are fixed to the results from the DFT-optimized model of the Si(100) surface and then scaled appropriately so as to fit on the STM image. These data conclusively show that the exo product is the experimentally observed product.

The real question that needs to be addressed is why the exo product is exclusively favored for room temperature reactions given that it is only 0.46 kcal/mol more stable than the endo product. In an analysis of over 1000 reacted sites there is no evidence whatsoever for the endo product.

In what follows, we introduce an algorithm that allows one to test for the presence of symmetry-allowed SOIs in the formation of cycloaddition products on the Si(100) surface and in turn to demonstrate that the predicted energetic influence of the SOIs is supported by DFT calculations. In the tradition of Woodward−Hoffmann we begin by first describing the frontier HOMO and LUMO levels of the reacting 1,3-CHD molecule, which are shown in Figure 3a and b, respectively. In addition to the orbital map showing the phase of the MOs we have labeled, in a plane parallel to the molecule, the positive lobes with a "1" and the negative lobes with a "0" such that each frontier orbital may be described by the binary matrix representation at the left of the figure.

In order to examine for possible frontier orbital interactions between the 1,3CHD molecule and the surface it is necessary to have knowledge of the phase information within the CWs that serves to build the frontier bands of the Si(100) surface. In a previous publication[13] we have shown via a DFT and Brillouin zone-folding technique, that the frontier bands appropriate for the lowest-energy c(4 × 2) Si(100) reconstruction are described by 16 ($8\pi$ and $8\pi^*$) high-symmetry crystal wave functions (CWs) each of which have each been plotted in Figure 3c. As in the case of the frontier molecular orbitals of 1,3-CHD, phase information within each of the Si(100) surface CWs can be represented as a binary matrix and full details are provided in the SI. Here we focus on just a single CW, the $\pi_1$J CW plotted out in Figure 4a where the rombohedral structure in the image represents the unit cell of the c(4 × 2) Si(100) reconstruction. We represent the phase information within the CW using the lowest-order regular matrix which is of dimension (4 × 8) and necessarily rotated with respect to the dimer row direction. For example, the phase information contained within the brown and yellow rectangles in Figure 4a (i.e., along the Si dimer row and dimerization directions, respectively) becomes the binary patterns on the left most column and bottom row of the matrix given in Figure 4b. In this manner, each of the 16 Si(100) CWs in Figure 3c can be transformed into a binary matrix (see SI).

Given a description for the phase information within the frontier wave functions appropriate for both molecule and surface we now examine, using a simple pattern search algorithm, whether frontier orbital interactions might indicate a preference for the endo or exo product in the reaction of 1,3CHD on Si(100). Specifically, our algorithm, when provided with a search matrix representing the HOMO or LUMO of the 1,3-CHD molecule and orientated with respect to the template matrix of the Si (100) CWs in the appropriate registry associated with the endo or exo adducts (i.e., the single bond between $C_2$ and $C_3$ atoms in the unreacted 1,3CHD molecule runs parallel to the Si dimer row direction), examines if there exists over an appropriate set of Si(100) CWs ($\pi$ or $\pi^*$ type) a phase-matched pattern. In the event that an identical pattern is located, signaling an entirety of favorable primary and secondary orbital interactions between the molecule and surface wave functions, the algorithm outputs the particular CW, whether it involves interaction with the molecular HOMO or LUMO level, and whether the registry of the favorable interaction corresponds to the endo or exo product. For clarity the operation of the search algorithm is shown

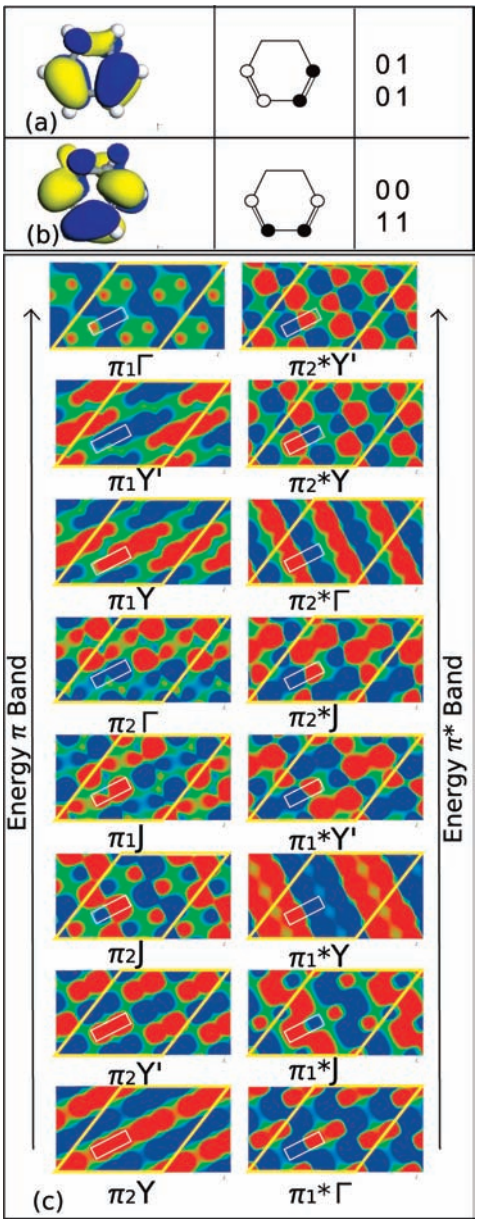


**Figure 3.** HOMO (a) and LUMO (b) with the corresponding binary representation of those frontier orbitals for the 1,3CHD molecule. (c) The 16 high symmetry crystal wave functions (CWs) that serve to construct the frontier bands of the c(4 × 2) Si(100) surface.[13] An individual Si dimer is indicated in each of the CWs with a white rectangle. The energy ordering of the CWs is indicated with the arrows to the left and right.

schematically in Figure 4c where the search and template matrices correspond to the 1,3-CHD LUMO and Si (100) $\pi_1J$ wave functions, respectively. Information returned from the pattern search can in turn be used to determine whether the pattern match has occurred over a Si dimer row or Si dimer valley and which of either the endo or exo reaction trajectories is likely to experience the greatest energy-lowering frontier orbital interactions en route to adduct formation.

Table 2 shows the output from the algorithm described above. The first column in the table indicates the type of interaction considered and specifies whether the pattern matching occurs between the molecular $\pi$ and the surface $\pi^*$ or vice versa

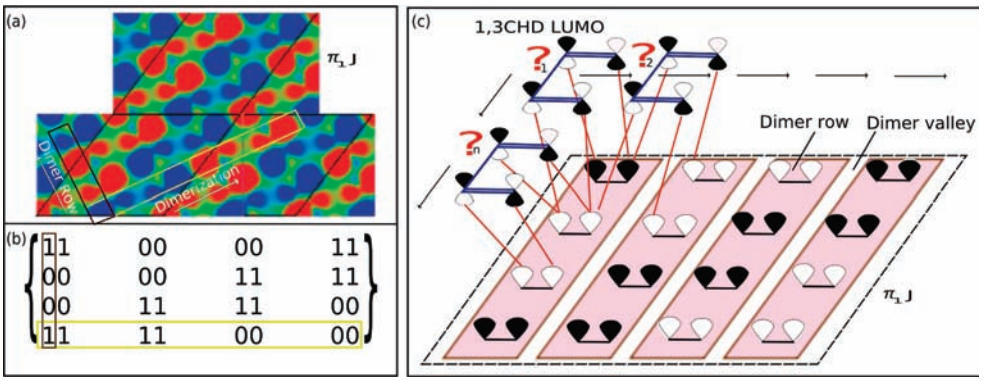


**Figure 4.** Schematics in (a) and (b) indicate how the phase information of a Si(100) $\pi$ CW is represented in a matrix. The phase information enclosed by the blue rectangle in the Si(100) $\pi_1$J CW becomes the bottom binary pattern in the (8 × 8) matrix given in (b). The workings of the search algorithm is indicated in (c). If phase information between the molecule and surface states is found to be commensurate, the algorithm will identify the CW and location of the pattern with respect to the underlying atoms and unit cell of the c(4 × 2) Si(100) surface. Note there are no commensurate matches established with either the endo or exo configurations of the molecule on the $\pi_1$J CW.

**Table 2. Truth table from the pattern search algorithm for adsorption of 1,3-CHD on Si(100) in the endo and exo configurations**

| interaction | match ? | CWs | configuration |
|---|---|---|---|
| Mol $\pi^*$, Sur $\pi$ | 0 | – | – |
| Mol $\pi$, Sur $\pi^*$ | 1 | $\pi_1^*\Gamma$ | exo |

(HOMO−LUMO or LUMO−HOMO). The second and third columns indicate the number of successful matches and the identity of the CW involved. The fourth column records the configuration of the molecule for which the pattern match was successful. The results show that there is no pattern match for the endo configuration of the molecule interacting with any of the Si(100) surface CWs. Thus, the endo configuration of the 1,3-CHD molecule is subject to unfavorable orbital interactions for every permutation of frontier wave function interactions. In contrast, the HOMO corresponding to the exo reaction configuration of the 1,3-CHD molecule is supported on the $\pi^*\Gamma$ CW of the Si(100) surface, and therefore, the molecule in this reaction configuration may experience favorable primary and secondary orbital interactions toward the eventual establishment of the exo product.

We now use DFT to examine in a qualitative fashion the frontier interaction between the 1,3-CHD molecule with the Si(100) surface prior to actual chemical bond formation. Figure 5 shows the result of a DFT analysis that maps out, in the absence of any atomic relaxations, the interaction energy of the surface−molecule system as a function of height above and lateral position along a defined axis perpendicular to the (2 × 1) dimer rows of the Si(100) surface. The calculations use the same substrate model and DFT parameters used to predict the total energy and LDOS differences between endo and exo products as described earlier (see SI). Note that for each of the 45 single-point energy calculations used to derive the contour map in Figure 5, the rotational orientation of the molecule with respect to the surface was constrained as indicated in the ball and stick model shown. This molecule−surface orientation was chosen such that the approach geometry of the unreacted 1,3-CHD molecule mimics either the endo or exo product geometry, depending on where precisely the molecule lands above the

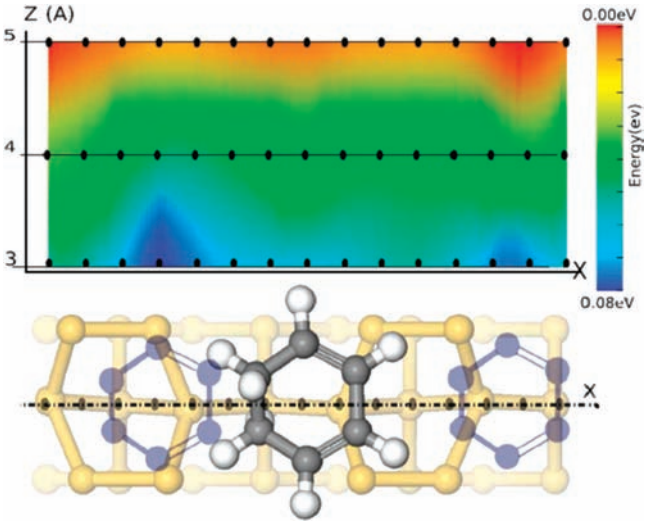


**Figure 5.** Contour map is the result of a DFT analysis that maps out, in the absence of any atomic relaxations, the interaction energy of the surface molecule system as a function of height ($z$) and displacement along the $x$ coordinate (dashed line). In each of the 45 coordinates sampled, the molecule is rotationally fixed with respect to the dimer row direction so as to mimic the endo or exo product geometry, depending upon where the molecule lands on the surface. The registry of the unreacted molecule consistent with the two minima found for small-molecule surface separation is evidence the that kinetics of the 1,3 CHD on Si(100) reaction is favoring exo rather than endo product formation.

Si(100) dimer row. The contour map shows two distinct energy mimima (both of which are associated with the exo product) for small ∼3 Å separations of the molecule above the surface with a net energy lowering of ∼0.08 eV compared to the separated system. We note that this energy is significantly larger than the actual energy difference (0.02 eV) between the final state endo and exo products. The different minima depths and locality with respect to a given dimer row reflect the different buckling orientation of dimers in neighboring rows. The registry of the molecule corresponding to these minima is shown above the contour plot in the ball and stick model by the two gray outlines of the 1,3-CHD molecule. Both minima position the 1,3-CHD

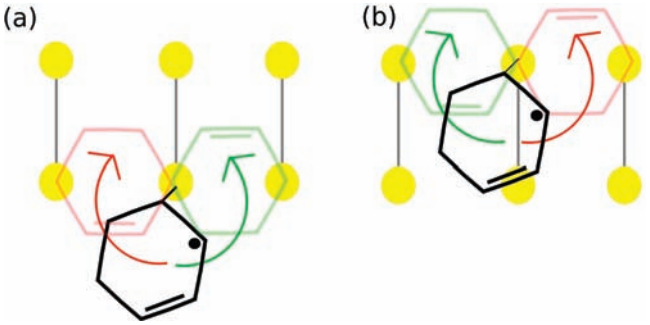


**Figure 6.** (a) and (b) Two orientations of a proposed 1,3CHD on Si(100) reaction intermediate tethered by a single Si−C bond to the Si(100) surface. In (a) the intermediate is drawn with the remaining C═C bond in the molecule orientated above the dimer valley. Clockwise and anticlockwise rotations about the Si−C bond lead to the exo (red) and endo (green) products respectively. In (b) the intermediate is drawn with the remaining C═C bond in the molecule orientated above the dimer row. From this orientation, clockwise and anticlockwise rotations about the Si−C bond lead to the endo and exo products, respectively. In the publication of Hayes et al.[4] it is argued on the basis of a series of molecular dynamics simulations that the exo reaction takes advantage of the degeneracy of pathways toward the exo product but that the endo reaction cannot.

molecule such that all unsaturated C−C bonds in the unreacted molecule lie over the dimer valley as opposed to the dimer row and thus support the presence of SOIs that favor exo product formation, consistent with the prediction of our frontier orbital algorithm.

Figure 5 demonstrates that the potential energy landscape above the Si(100) surface favor molecules that react to yield the exo product. The presence of these long-range steering interactions is a manifestation of SOIs and a validation of the symmetry-based algorithm proposed in this work. However, even though the corrugation in the energy landscape (0.08 eV) is larger than the absolute energy differences between the product (0.02 eV) it still cannot account for the exclusive formation of the exo product. Clearly, there are still missing ingredients that must be uncovered to better understand the chemical dynamics of this system.

Although this analysis points to the likely role of SOIs is guiding product formation through a concerted reaction mechanism, other researchers have attempted to explain the product distribution by evoking reaction intermediates. For example Hayes et al.,[4] used molecular dynamics calculations to simulate the reaction of 1,3-CHD on Si(100) and predicted a population ratio of endo:exo ($C_t$: $C_r$ in ref 4) of ∼1:3. These authors argued, that the high population of type *C* products (the exo and endo product class) despite being thermodynamically disfavored, can be explained if a common step in each of the reaction pathways is the formation of a radical intermediate bound by one Si−C bond. The authors reason that, from this intermediate, the reaction toward product type *C* would be promoted due to the availability of reactive Si sites either side of and adjacent to the Si atom of initial attachment and that the higher degeneracy in reaction pathways for this product type promotes it above the alternative thermodynamically favored products. This rationale cannot, however, discriminate between the endo and exo products that are stereoisomers of one another since rotations about the Si−C bond of the intermediate would facilate endo and exo formation with equal probability (see Figure 6). Moreover, whether the reaction is truly concerted or asymmetric, is not known, but the steering effect described in this work must be accounted for in the reaction dynamics and will inevitably result in a significant predisposition toward exo product formation.

In conclusion, we have shown through this DFT analysis that, as in the case of homogeneous reactions, surface product distributions cannot always be explained by a thermodynamics analysis. In the case of the reaction of 1,3-CHD with Si(100), secondary orbital interactions play an important role in kinetically destabilizing the endo transition state relative to that of the exo product. We expect that these SOIs are likely important in a wide range of surface chemical phenomena and that the search algorithm introduced here and supported by DFT calculations will be a useful tool in analysis of the surface reaction product distributions.

## ■ ASSOCIATED CONTENT

**Supporting Information.** Full computational details and the optimized structures for the endo and exo models; a selection of other DFT methodologies and details of these additional calculations; binary representations of the 16 CWs appropriate to represent the frontier crystal wave functions of the *c*4 × 2 Si(100) 2 × 1 surface. This material is available free of charge via the Internet at http://pubs.acs.org/.

## ■ AUTHOR INFORMATION

**Corresponding Author**
jboland@tcd.ie

## ■ ACKNOWLEDGMENT

Trinity Center for High Performance Computing and the financial support of Science Foundation Ireland (Grant No. 06/IN.1/I106) are gratefully acknowledged. We also thank Dr. Gino Di Labio at the University of Alberta, Edmonton, Canada for his help in analysis of DFT data.

## ■ REFERENCES

(1) Filler, M. A.; Bent, S. F. *Prog. Surf. Sci.* **2003**, *73*, 1–5610.1016/S0079-6816(03)00035-2.
(2) Wolkow, R. A. *Annu. Rev. Phys. Chem.* **1999**, *50*, 413.
(3) Suzuki, T.; Sorescu, D. C.; Yates, J. J. T. *Surf. Sci.* **2006**, *600*, 5092–5103.
(4) Hayes, R. L.; Tuckerman, M. E. *J. Am. Chem. Soc.* **2007**, *129*, 12172–12180.
(5) Minary, P.; Tuckerman, M. E. *J. Am. Chem. Soc.* **2005**, *127*, 1110–1111.
(6) Teague, L. C.; Boland, J. J. *J. Phys. Chem. B* **2003**, *107*, 3820–3823.
(7) Teague, L. C.; Chen, D.; Boland, J. J. *J. Phys. Chem. B* **2004**, *108*, 7827–7830.
(8) Choi, C. H.; Gordon, M. S. *J. Am. Chem. Soc.* **1999**, *121*, 11311–11317.
(9) Konecny, R.; Doren, D. J. *J. Am. Chem. Soc.* **1997**, *119*, 11098–11099.
(10) Lee, H. S.; Choi, C. H.; Gordon, M. S. *J. Am. Chem. Soc.* **2005**, *127*, 8485–8491.
(11) Hoffmann, R.; Woodward, R. B. *J. Am. Chem. Soc.* **1965**, *87*, 4388–4389.
(12) Hoffmann, R.; Woodward, R. B. *The Conservation of Orbital Symmetry*; Academic Press: New York, 1969.
(13) Ryan, P. M.; Teague, L. C.; Boland, J. J. *J. Am. Chem. Soc.* **2009**, *131*, 6768–6774.

(14) Segall, M. D.; Lindan, P. J. D.; Probert, M. J.; Pickard, C. J.; Hasnip, P. J.; Clark, S. J.; Payne, M. C. *J. Phys.: Condens. Matter* **2002**, *14*, 2717–2744.
(15) Hayes, R. L.; Tuckerman, M. E. *J. Phys. Chem. C* **2010**, *114*, 15102–15108.